

**Libra Workshop and Summer School on Excited States and
Nonadiabatic Dynamics 2024**



Nonadiabatic Dynamics in Metal Halide Perovskites

Wei Li (李位)

School of Chemistry and Materials Science
Hunan Agricultural University

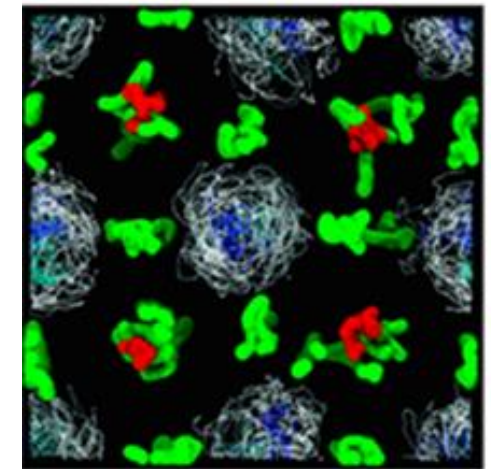
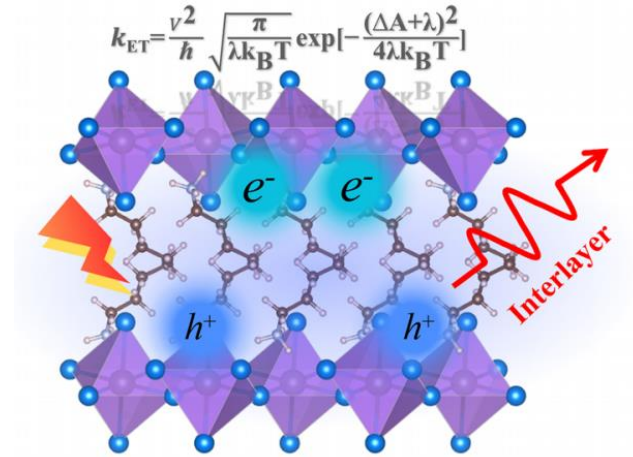
Outline

1. Theoretical methodologies:

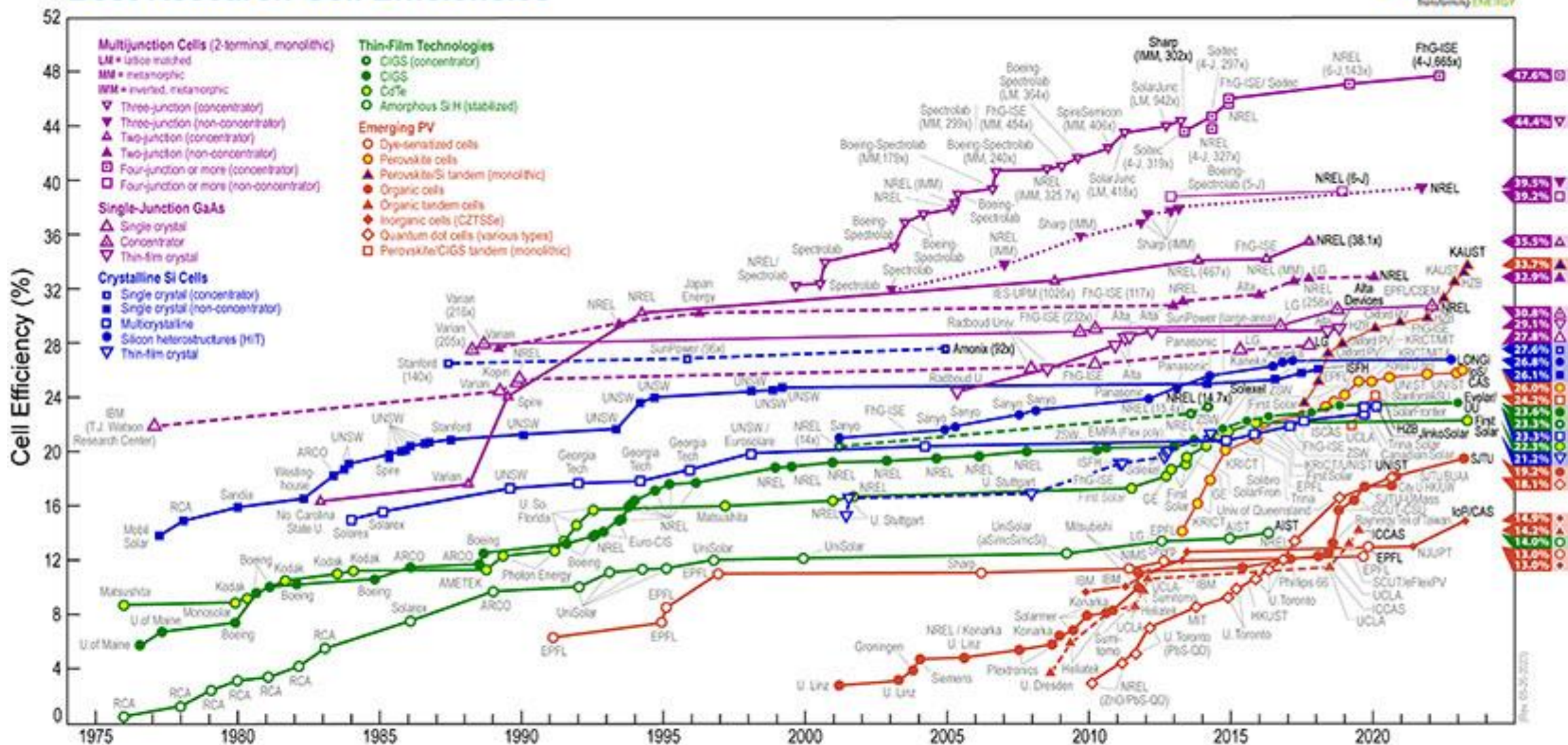
- Interlayer carrier dynamics in 2D perovskites.
- Spin-orbital coupling in nonadiabatic dynamics.
- Hamiltonian repetition method for long-time nonadiabatic dynamics.

2. Why can quantum dynamics teach about perovskites:

- Why many defects are benign?
- Mechanisms of defect passivation.
- Unusual T and P dependence.

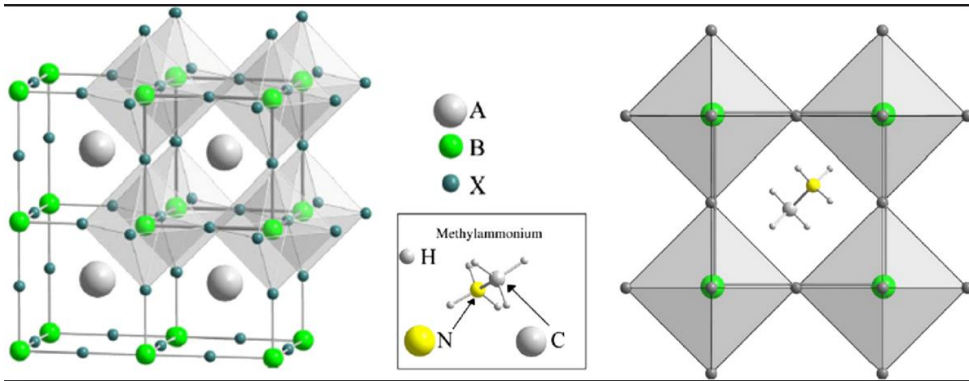


Best Research-Cell Efficiencies



3D/2D Perovskites

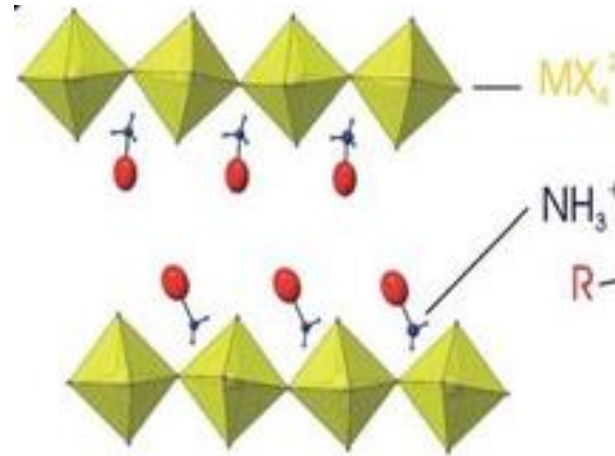
Generic formula: ABX_3 , BX_6 octahedral
 $CH_3NH_3PbI_3$



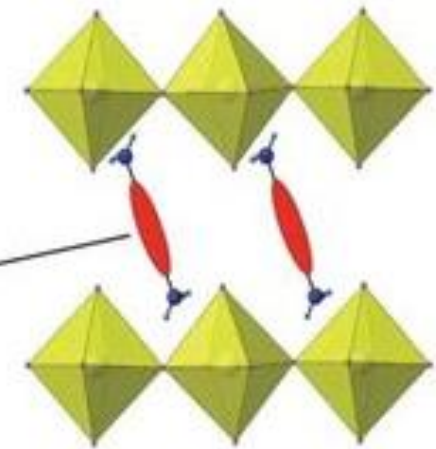
- ✓ Low exciton binding energy, ~19 meV
- ✓ Long carrier diffusion length
- ✓ High absorption coefficients
- ✓ Low recombination rate

× stability issue (Humidity, Light, Thermal)

Ruddlesden-Popper
 $(RNH_3)_2A_{n-1}B_nX_{3n+1}$

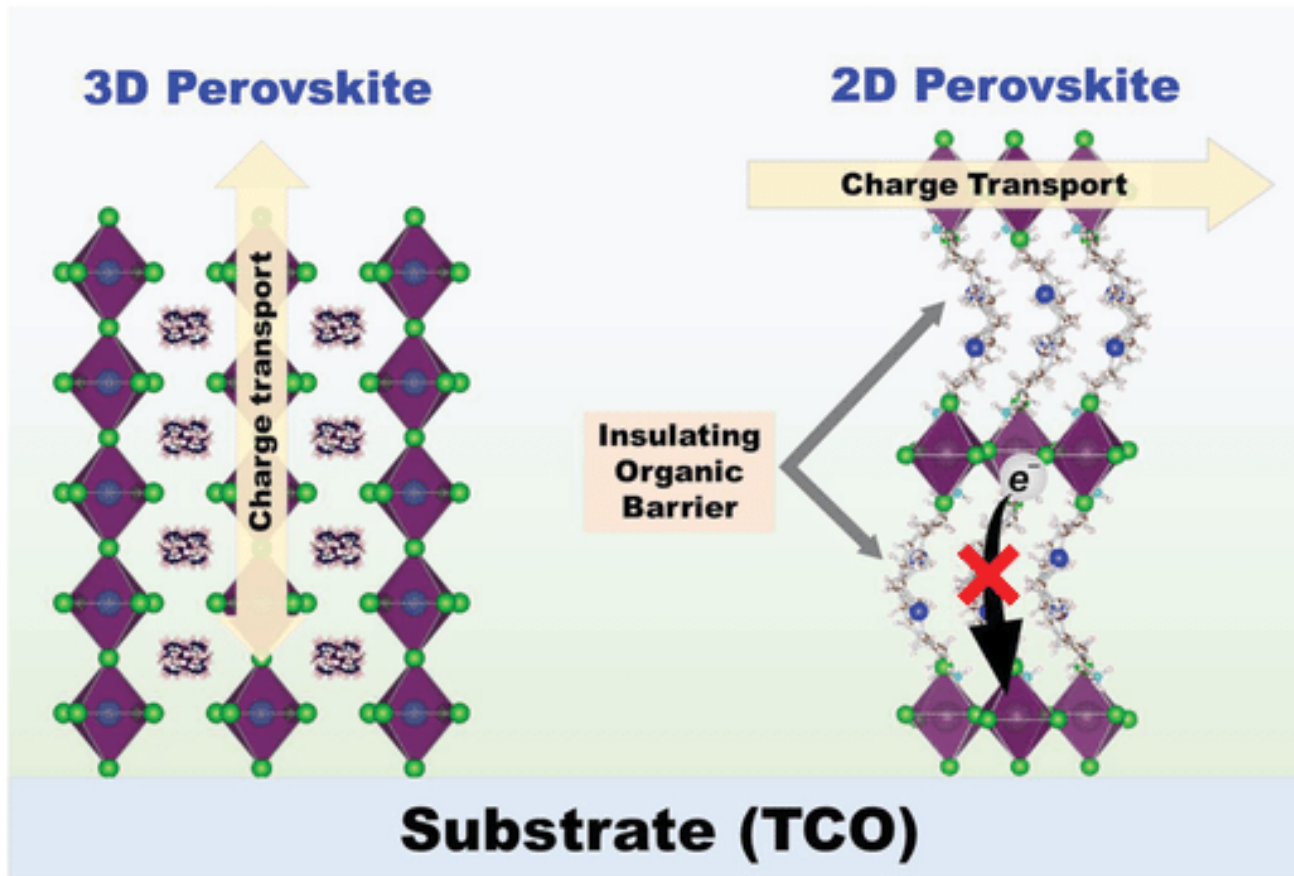


Dion-Jacobson
 $R(NH_3)_2A_{n-1}B_nX_{3n+1}$

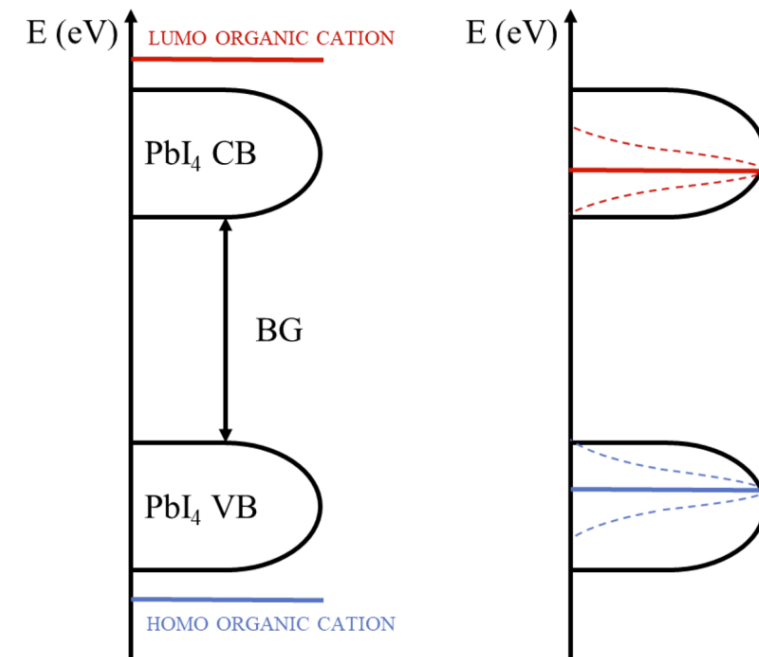


- ✓ High stability (Hydrophobicity of spacer cations)
- ✓ Structural tunability

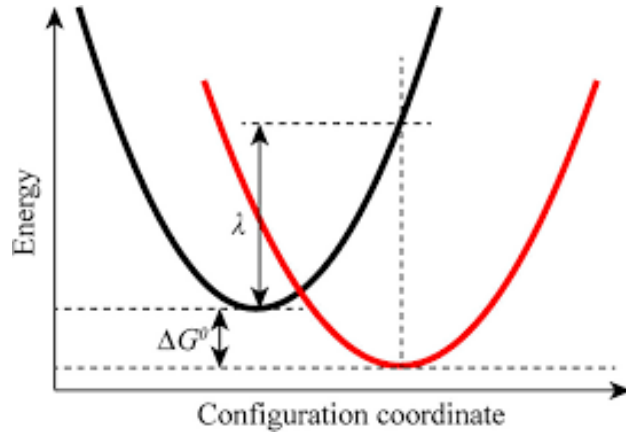
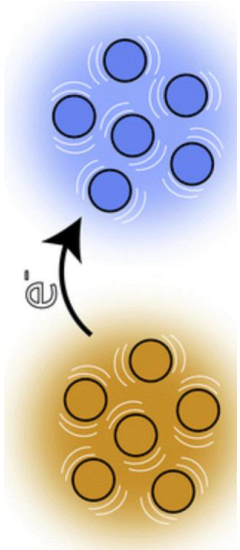
Interlayer Charge Transport in 2D Perovskites



The interlayer charge transfer is limited by the insulating nature of spacer cations!



Marcus Electron Transfer



V_{kl} : diabatic coupling between localized states
(non-local electron-phonon coupling)

λ : reorganization energy (local electron-phonon coupling)

ΔG : barrier height, zero for equivalent layer

Methods for diabaticization:

- block diagonalization
- generalized Mulliken-Hush method
- fragment charge difference
- fragment energy difference
- projection methods
- fragment orbital density functional theory
- constrained density functional theory
- block-localized wavefunction theory

$$k_{Marcus} = \left(\frac{V_{kl}^2}{\hbar} \right) \sqrt{\frac{\pi}{\lambda k_B T}} \exp \left(-\frac{\Delta G + \lambda}{4k_B T} \right)$$

$$\frac{J(\omega)}{\omega} = \frac{1}{2k_B T} \int_0^\infty \langle \delta\Delta E(0) \delta\Delta E(t) \rangle_M \cos \omega t$$

$$\lambda = \frac{2}{\pi} \int_0^\infty \frac{J(\omega)}{\omega} d\omega$$

Projection-operator Diabatization (POD) Approach

- **Kohn-Sham Hamiltonian** expressed in terms of **orthogonalized atomic orbital** basis set is partitioned in **donor** and **acceptor** blocks
- **coupling matrix** between donor and acceptor states are identified **transformed** matrix elements of the **off-diagonal block**

$$\psi^{\mathbf{k}}(\mathbf{r}) = \frac{1}{\sqrt{N}} \sum_n e^{i\mathbf{k}\mathbf{R}_n} \sum_i c_i^{\mathbf{k}} \phi_i^{\mathbf{k}}(\mathbf{r} - \mathbf{R}_n)$$

The Bloch function can be expressed as linear combination of atomic orbital basis

$$H^{\mathbf{k}} = \sum_n e^{i\mathbf{k}\mathbf{R}_n} \langle \phi_i(\mathbf{r}) | H | \phi_j(\mathbf{r} - \mathbf{R}_n) \rangle$$

$$S^{\mathbf{k}} = \sum_n e^{i\mathbf{k}\mathbf{R}_n} \langle \phi_i(\mathbf{r}) | S | \phi_j(\mathbf{r} - \mathbf{R}_n) \rangle$$

Löwdin symmetric procedure:

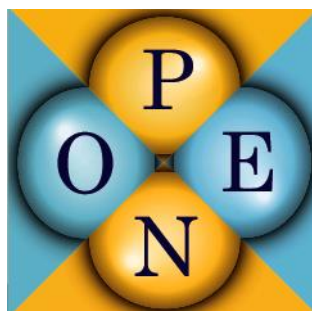
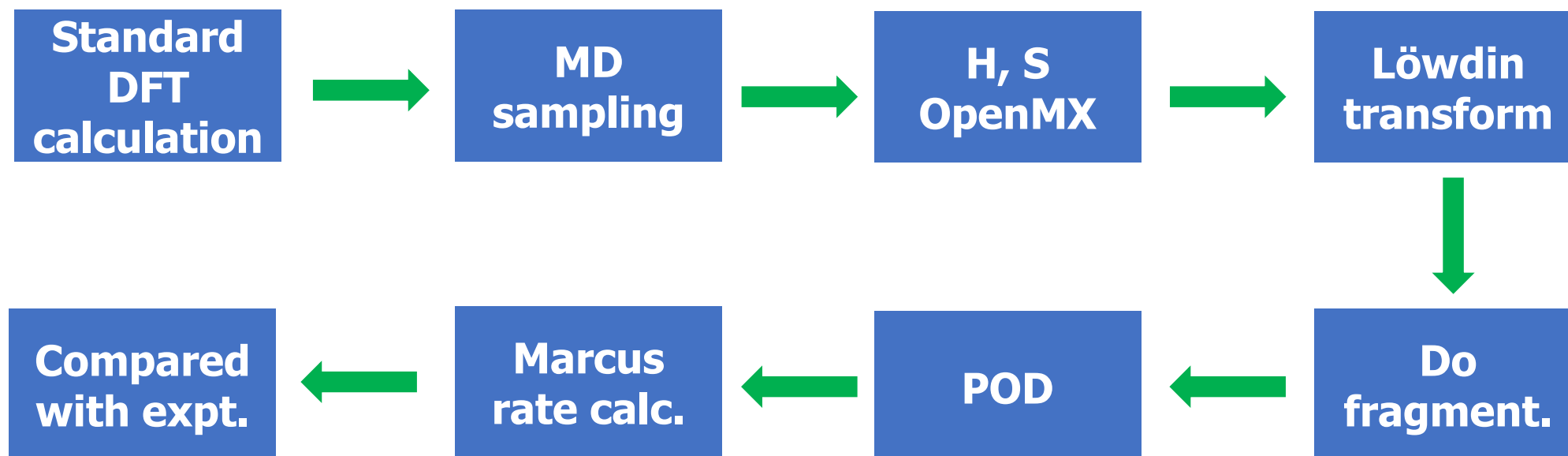
$$|\tilde{\phi}_i\rangle = \sum_j S_{ji}^{1/2} |\phi_j\rangle \quad \tilde{H} = S^{-1/2} H S^{-1/2}$$

Diabatic energy:

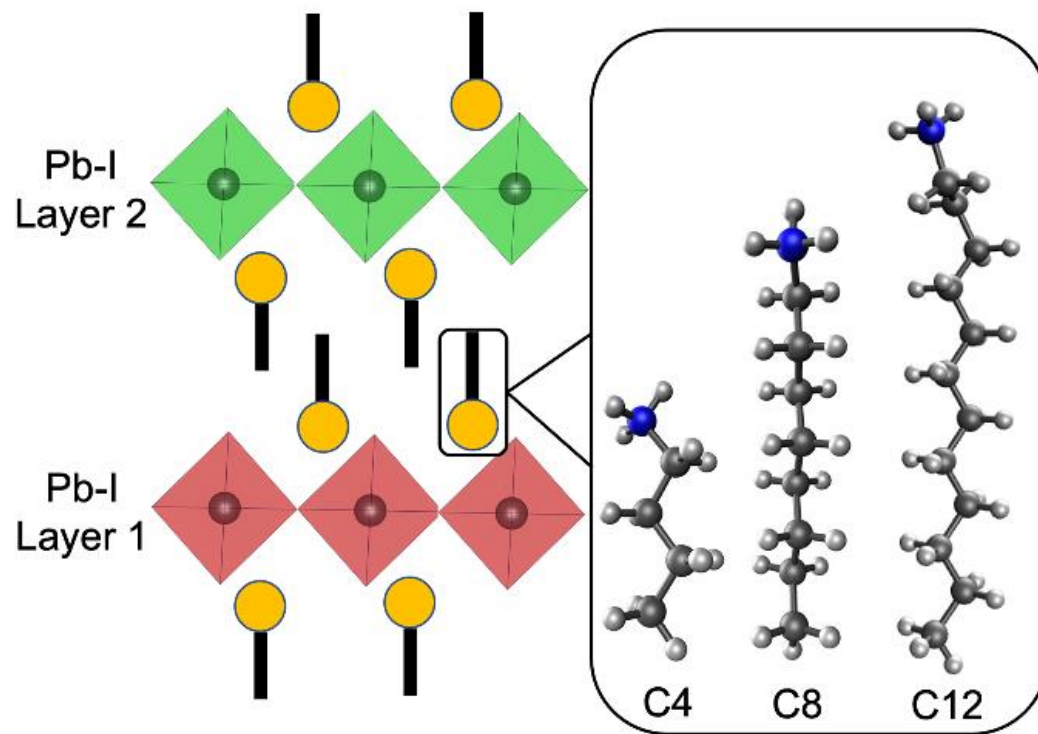
$$\varepsilon_{DD} = T_D^+ \tilde{H}_{DD} T_D; \quad \varepsilon_{AA} = T_A^+ \tilde{H}_{AA} T_A$$

$$T_A^+ \begin{bmatrix} \tilde{H}_D & \tilde{H}_{DA} \\ \tilde{H}_{AD} & \tilde{H}_A \end{bmatrix} T_D = \begin{bmatrix} \varepsilon_D & V_{DA} \\ V_{AD} & \varepsilon_A \end{bmatrix}$$

Workflow: interfacing with OpenMX



Alkyl Length-dependent Interlayer Charge Transfer

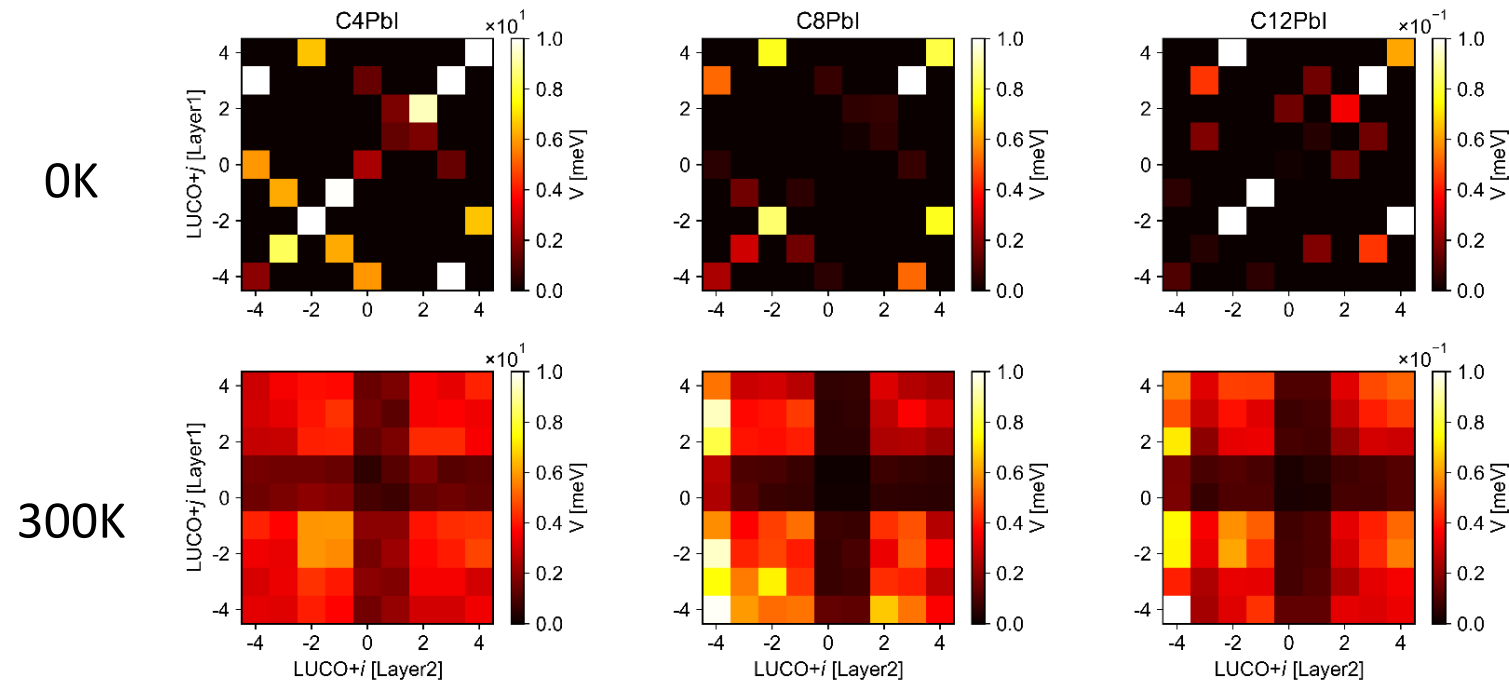


Ye et al., Nature Comm., 2020, **11**, 5481

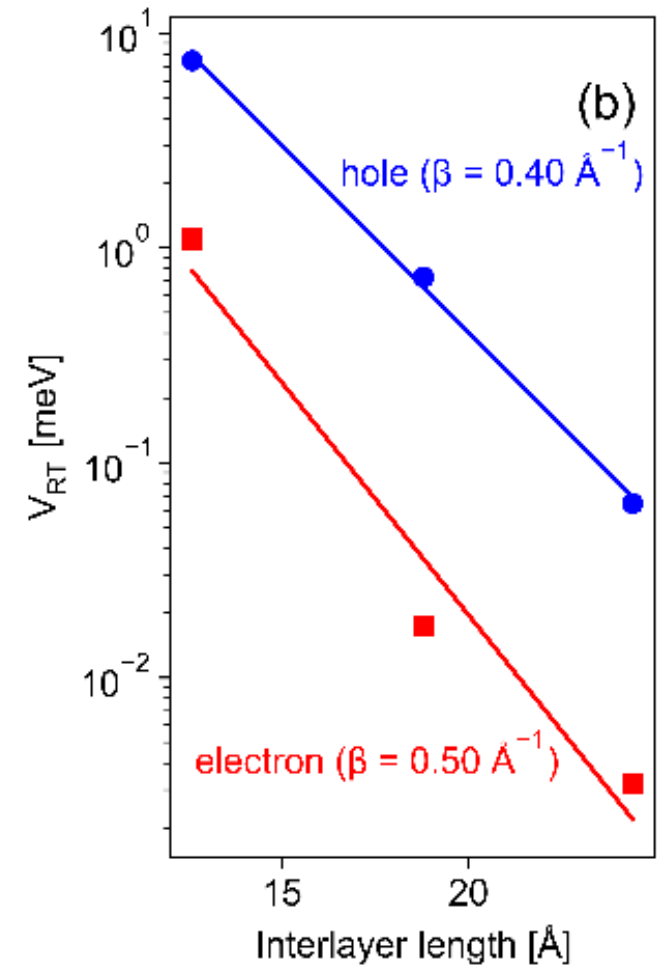
Boeije et al. J. Am. Chem. Soc. 2023, **145**, 21330

J. Comput. Theory Chem., 2023, **19**, 9403

Charge Transfer Couplings



- Hole transfer coupling is larger than electron transfer coupling
- Thermal fluctuation enhances the electronic coupling
- Longer organic cations decrease the electronic coupling



Electron and Hole Hopping Time

Table 1. Parameters for Interlayer Charge Transfer Computed for the Investigated 2D Layered Perovskites and Corresponding Transition Rates and Mobilities^a

| | | V_{kl} (meV) | $\langle V_{kl}^2 \rangle^{1/2}$ (meV) | σ_V (meV) | λ (eV) | τ_{Marcus} | μ_{hop} (cm ² V ⁻¹ s ⁻¹) |
|--------|---|-----------------------|--|-----------------------|----------------|------------------------|---|
| C4PbI | L | 8.7×10^{-2} | 1.10 | 1.08 | 0.83 | 137.6 ns | 4.46×10^{-6} |
| | H | 0.36 | 7.44 | 7.41 | 1.08 | 38.5 ns | 1.59×10^{-5} |
| C8PbI | L | 1.38×10^{-4} | 1.73×10^{-2} | 1.72×10^{-2} | 0.97 | 2.3 ms | 6×10^{-10} |
| | H | 1.98×10^{-3} | 0.73 | 0.65 | 0.54 | 18.8 ns | 7.35×10^{-5} |
| C12PbI | L | 4.34×10^{-5} | 3.2×10^{-3} | 3×10^{-3} | 1.18 | 572.0 ms | 3.99×10^{-12} |
| | H | 3.95×10^{-3} | 6.46×10^{-2} | 6.43×10^{-2} | 1.11 | 690.2 μ s | 3.31×10^{-9} |

^aHOCO–HOCO (H) and LUCO–LUCO (L) electronic couplings for the 0 K structures (V_{kl}) and canonically averaged electronic couplings from the MD simulations ($\langle V_{kl}^2 \rangle^{1/2}$), along with its standard deviation (σ_V); the averaged reorganization energy (λ); the hole and electron hopping time obtained from Marcus theory (τ_{Marcus}); and the carrier mobility calculated based on the Marcus hopping rate (μ_{hop}).

CPA for NA-MD based on constrained DFT

$$i\hbar \frac{\partial \psi(\mathbf{r}, t; \mathbf{R})}{\partial t} = H_e(\mathbf{r}, t; \mathbf{R}) \psi(\mathbf{r}, t; \mathbf{R})$$

$$\psi(\mathbf{r}, t; \mathbf{R}) = \sum_l c_l(t) \phi_l(\mathbf{r}; \mathbf{R}(t))$$

Expanding adiabatic wavefunction in fragment orbital basis

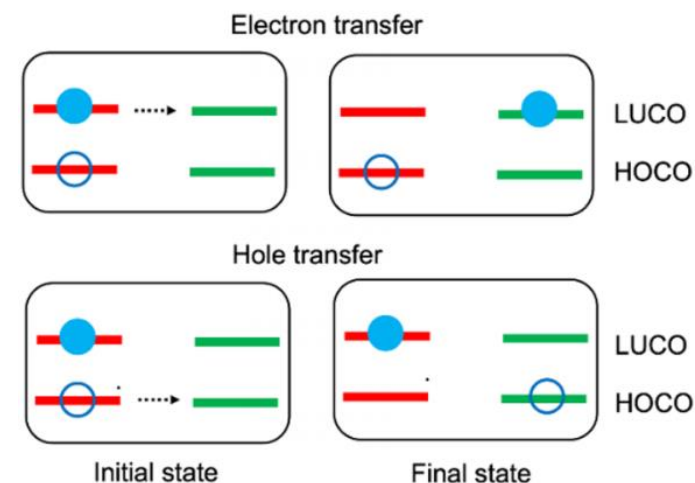
$$i\hbar \sum_l \frac{\partial c_k(t)}{\partial t} = \sum_l H_{vib,kl}(t) c_l(t)$$

$$H_{vib,kl} = H_{kl} - i\hbar \mathbf{d}_{kl}$$

If we consider H->H; L->L transitions

$$H_{kl} = \langle \phi_k | H | \phi_l \rangle$$

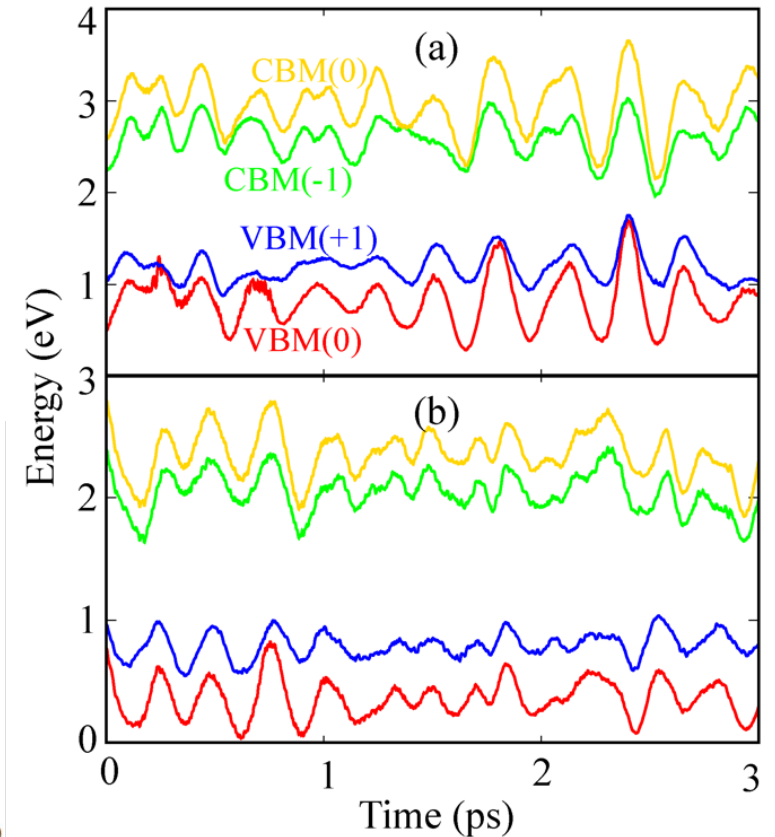
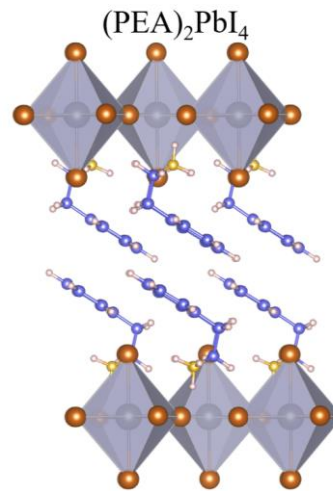
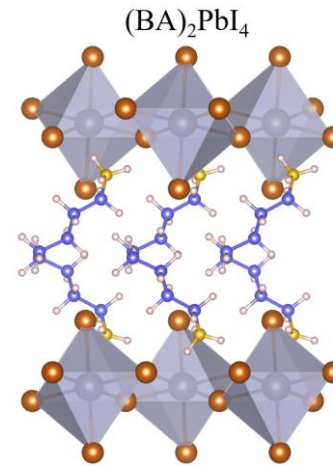
The key is to obtain the donor-acceptor energy splitting



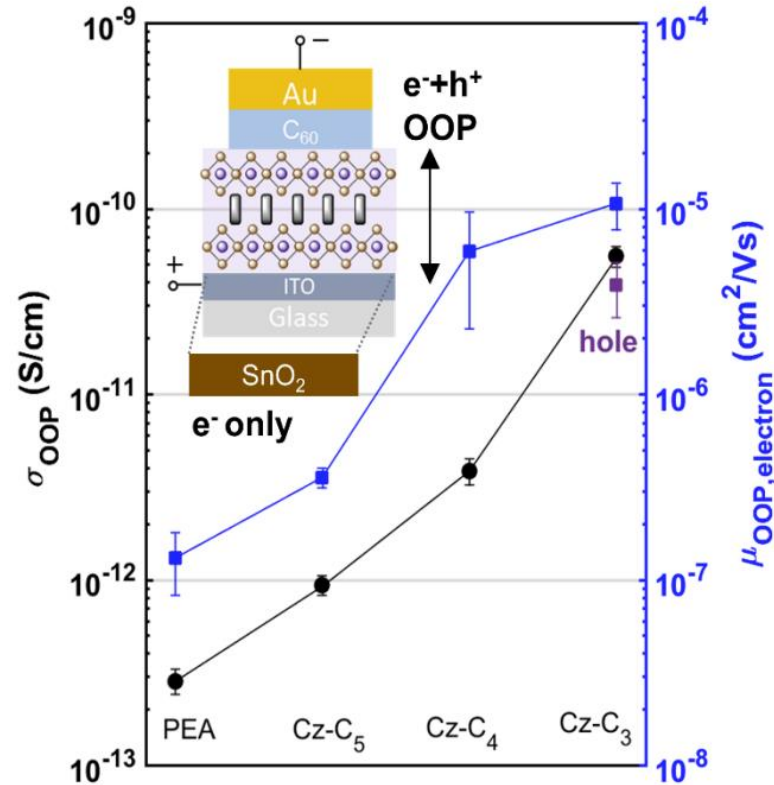
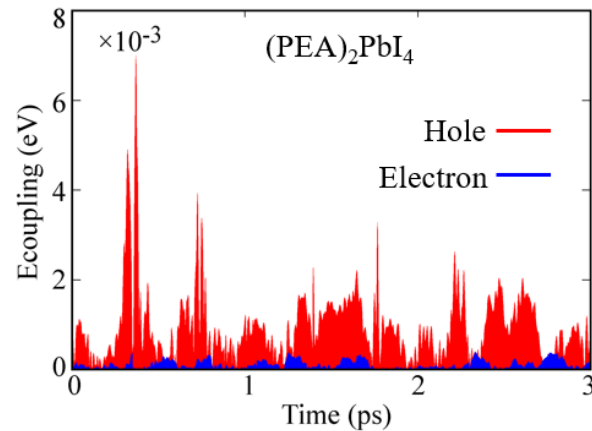
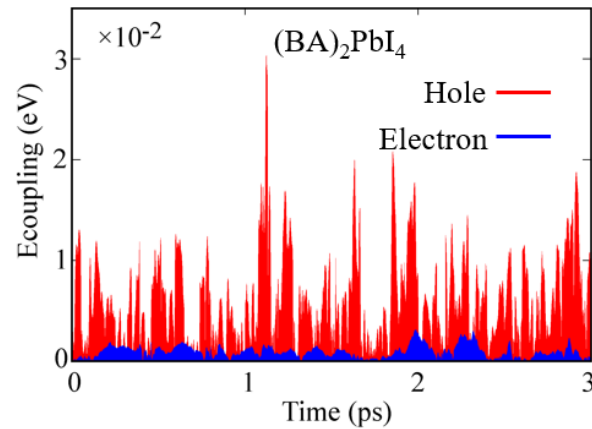
- **Insider layer**, electronic coupling is zero, basis is orthogonal; but NAC is non-zero
- **Between layers**, electronic coupling is non-zero; but NAC vanishes

CPA for NA-MD based on constrained DFT

- The excited state is approximately by perturbation of ground state charge density.
- The charge is constrained at one layer through adding/removing electrons and then hop to another layer.
- The splitting between donor and acceptor site energies characterizes the ET process within the two state picture.



CPA for NA-MD based on constrained DFT



PEA has 10^{-6} - 10^{-7} $\text{cm}^2/\text{V}/\text{s}$ out-of-plane carrier mobility, this gives 100 ns – 1 us hopping time

$$\mu_{\text{hop}} = \frac{eD}{k_B T} = \frac{ek_{\text{Marcus}} L^2}{k_B T}$$

CPA for NA-MD based on constrained DFT

| | | $\langle V^2 \rangle^{1/2}$ (meV) | λ (eV) | τ_{Marcus} | τ_{DISH} | D_{COM} (Å) | μ_{Marcus} (cm ² /V/s) | μ_{DISH} (cm ² /V/s) |
|--------|---|--------------------------------------|-------------------|-----------------|---------------|------------------|--|--|
| BAPbI | L | 1.10 | 0.83 | 137.6 ns | 24.0ns | 12.6 | $4.46 \cdot 10^{-6}$ | $2.6 \cdot 10^{-5}$ |
| | H | 7.44 | 1.08 | 38.5 ns | 5.2ns | | $1.59 \cdot 10^{-5}$ | $1.2 \cdot 10^{-4}$ |
| PEAPbI | L | 0.13 | 0.66 | 1.7 us | 17.9μs | 15.94 | $5.8 \cdot 10^{-7}$ | $5.5 \cdot 10^{-8}$ |
| | H | 0.27 | 0.60 | 210 ns | 5.3μs | | $4.7 \cdot 10^{-6}$ | $1.8 \cdot 10^{-7}$ |

Spin-orbit Interactions in Nonadiabatic Dynamics

$$(\hat{h}^{\text{KS}} + \hat{h}^{\text{SOC}})\psi_i^{\text{adi}} = \epsilon_i^{\text{adi}}\psi_i^{\text{adi}}$$

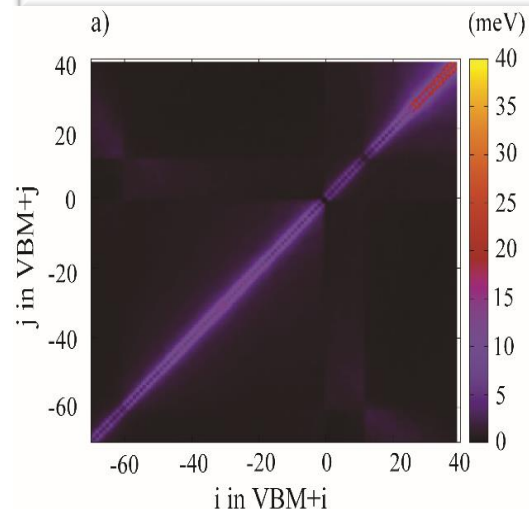
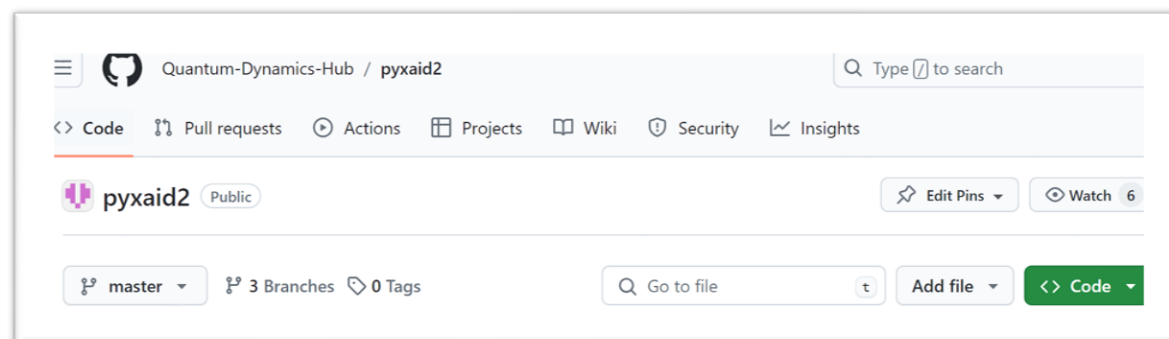
$$\psi_i = \phi_i^\alpha \alpha + \phi_i^\beta \beta = \begin{pmatrix} \phi_i^\alpha \\ \phi_i^\beta \end{pmatrix}, \quad i = 1, \dots, N$$

$$d_{ij}\left(t + \frac{dt}{2}\right) \equiv \frac{\langle \Phi_i(t) | \Phi_j(t + dt) \rangle - \langle \Phi_i(t + dt) | \Phi_j(t) \rangle}{2dt}$$

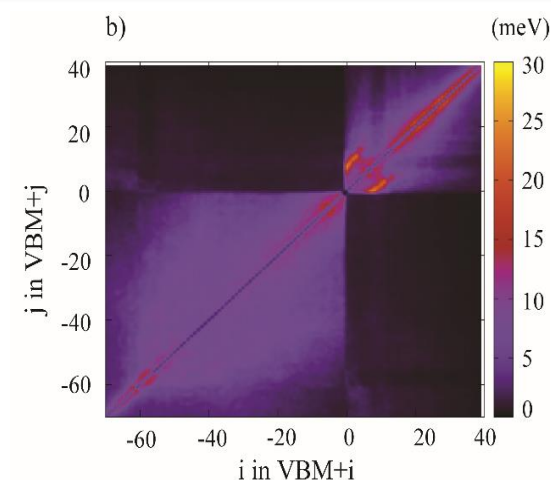
$$\begin{aligned} \langle \psi_i(t) | \psi_j(t') \rangle &= (\phi_i^\alpha(t) \phi_j^\beta(t)) \begin{pmatrix} \phi_j^\alpha(t') \\ \phi_j^\beta(t') \end{pmatrix} \\ &= \langle \phi_i^\alpha(t) | \phi_j^\alpha(t') \rangle + \langle \phi_i^\beta(t) | \phi_j^\beta(t') \rangle \end{aligned}$$

ACS Energy Lett., 2018, 3, 2159

Wavefunctions are expressed as two-component spinors



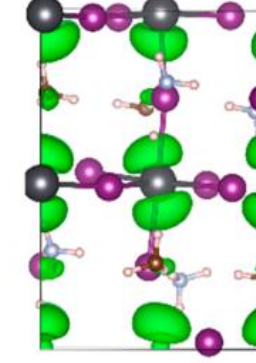
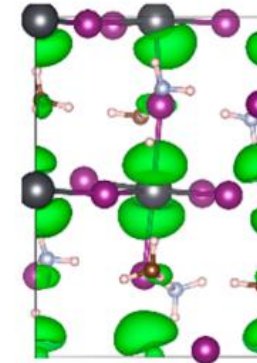
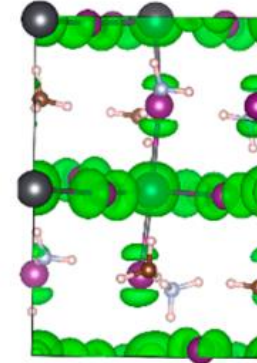
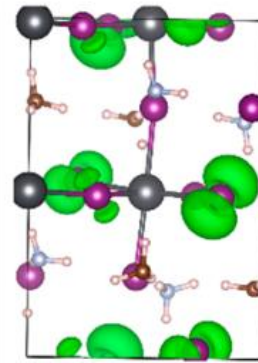
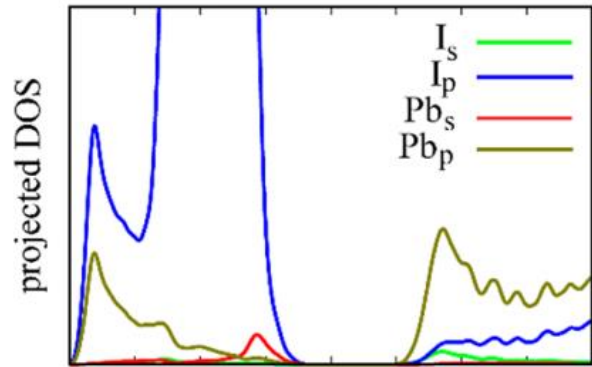
Without SOC



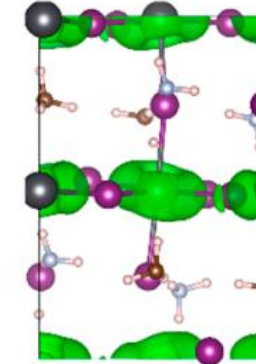
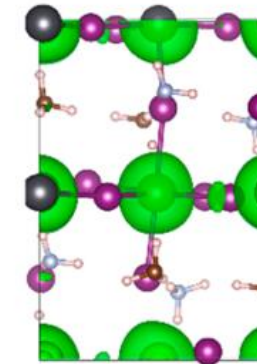
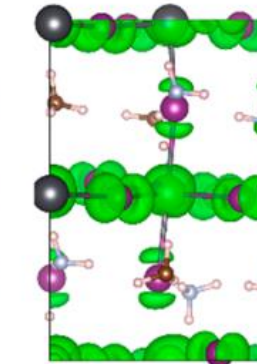
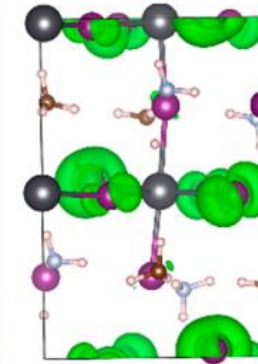
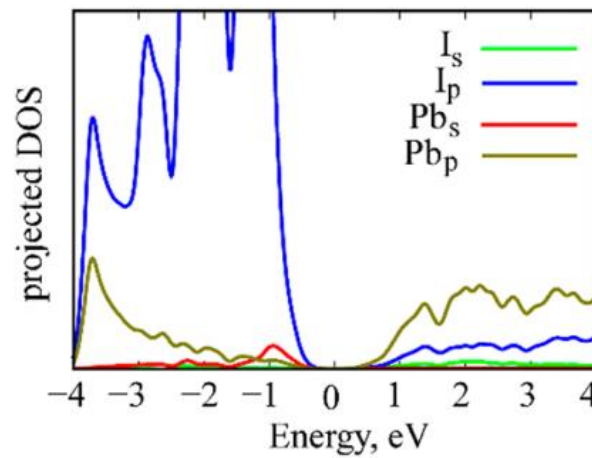
With SOC

Spin-orbit Interactions in Nonadiabatic Dynamics

Without SOC



With SOC



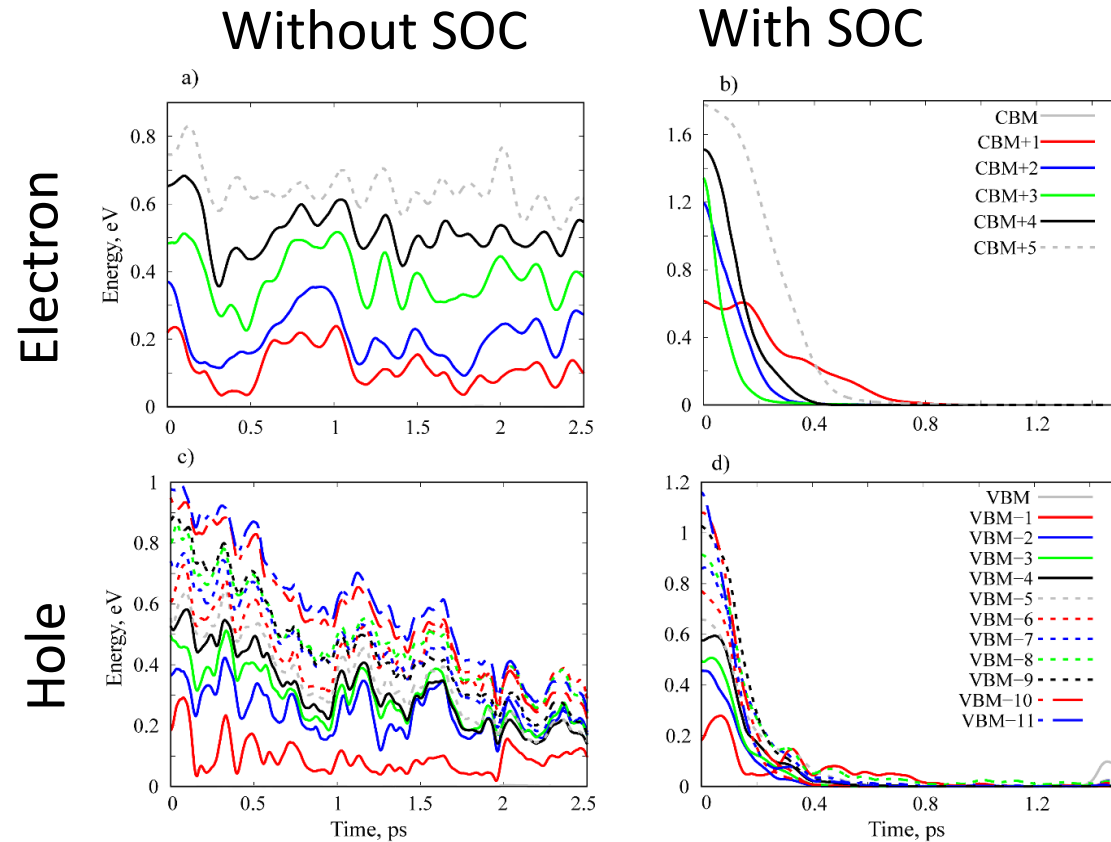
VBM-11

VBM

CBM

CBM+5

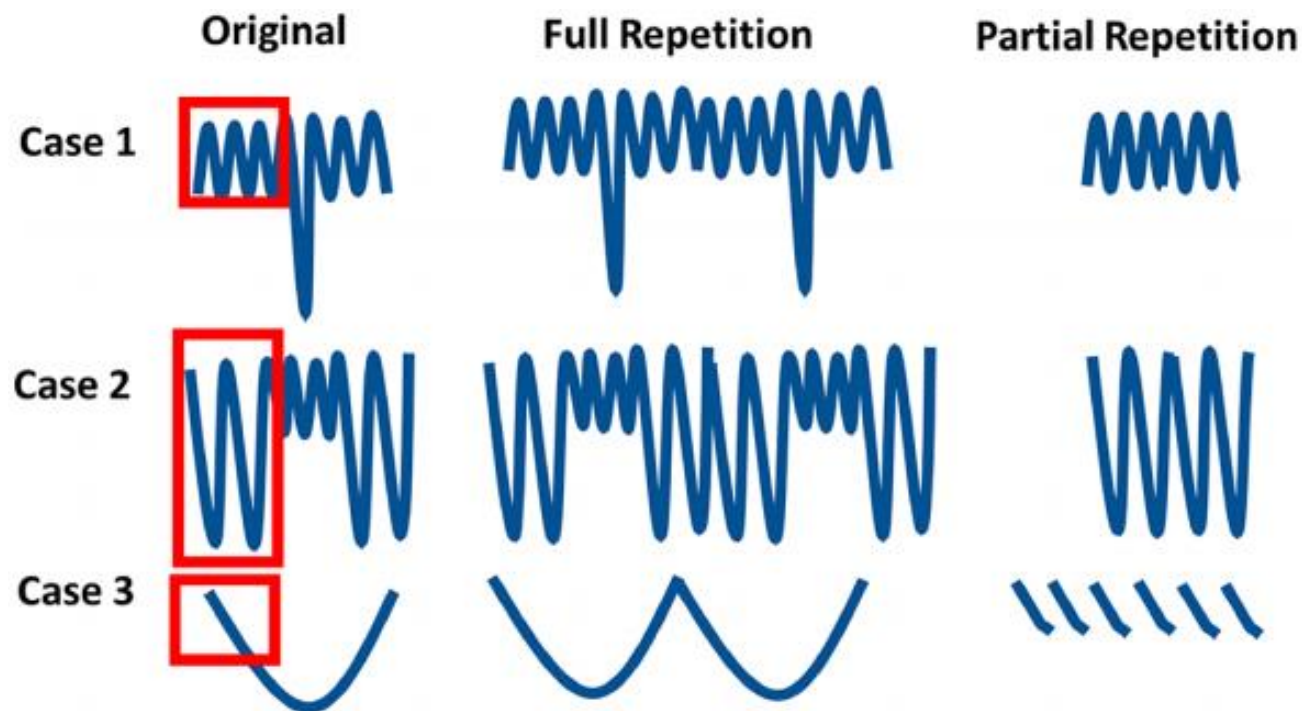
Spin-orbit Interactions in Nonadiabatic Dynamics



- Hole relaxation faster than electron relaxation - denser DOS for holes
- Spin-orbit interaction greatly speeds up relaxation - larger NA coupling

Hamiltonian Repetition in Nonadiabatic Dynamics

Repetition should capture the essential feature of the Hamiltonian

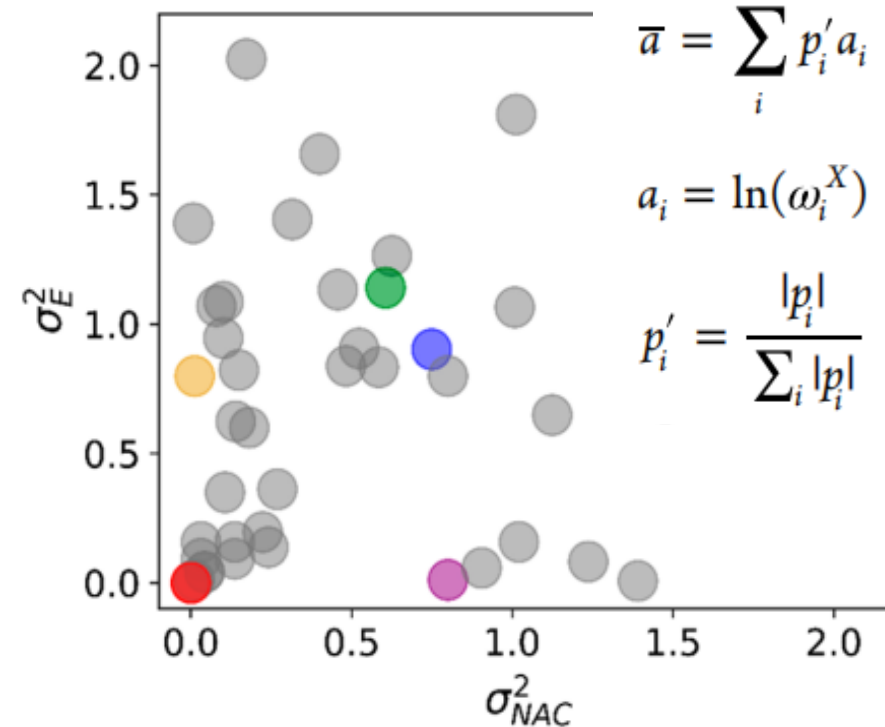


$$\sigma_X^2 = \sum_i p'_i (a_i - \bar{a})^2$$

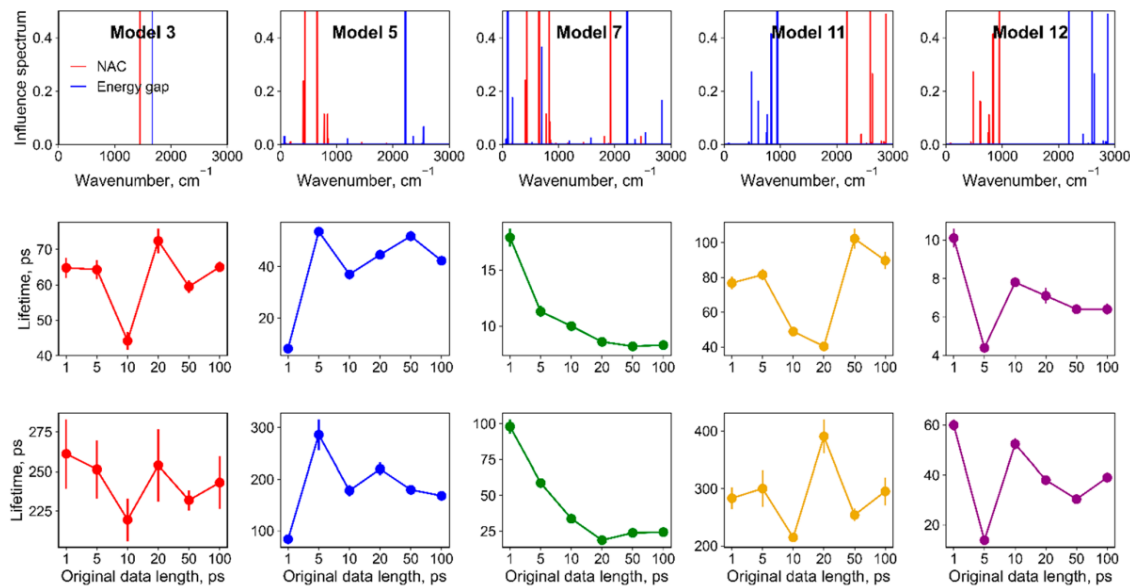
$$\bar{a} = \sum_i p'_i a_i$$

$$a_i = \ln(\omega_i^X)$$

$$p'_i = \frac{|p_i|}{\sum_i |p_i|}$$

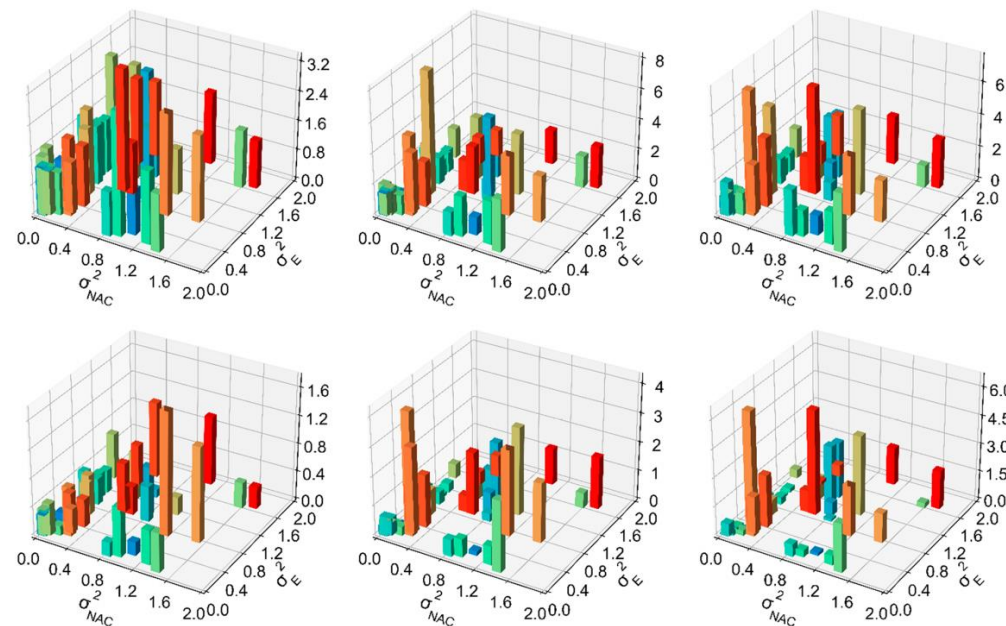


Hamiltonian Repetition in Nonadiabatic Dynamics



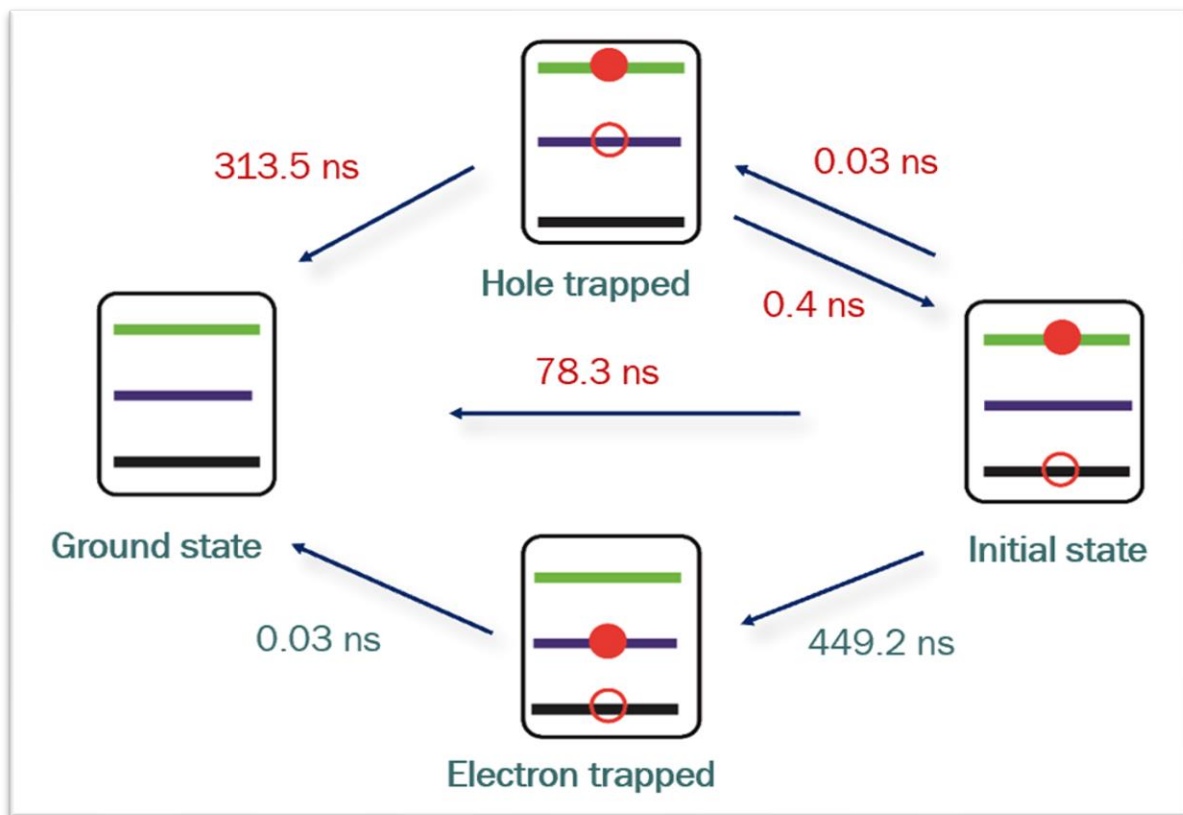
Convergence hard to achieve for the data sets involving low-frequency modes

The repetition approach becomes inaccurate in simulations with very small NACs



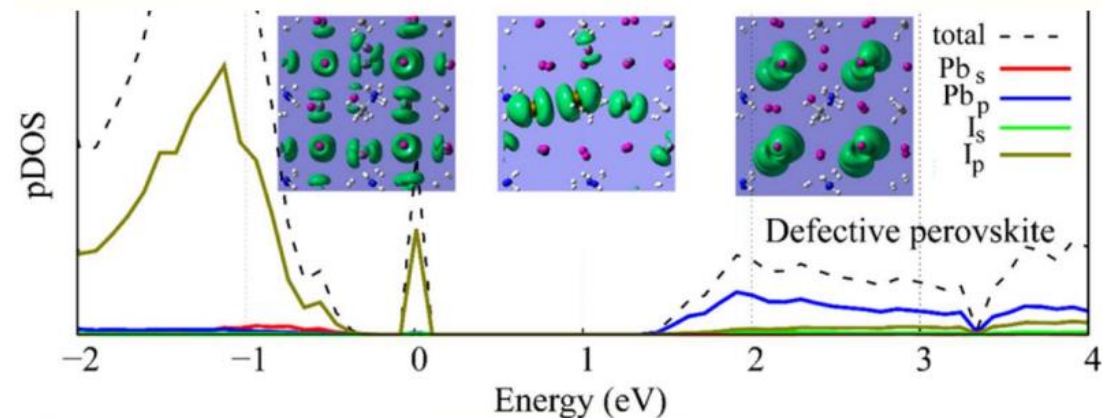
The overestimation or underestimation does not directly depend on the dispersion of frequencies

Iodine Interstitials Suppress Recombination

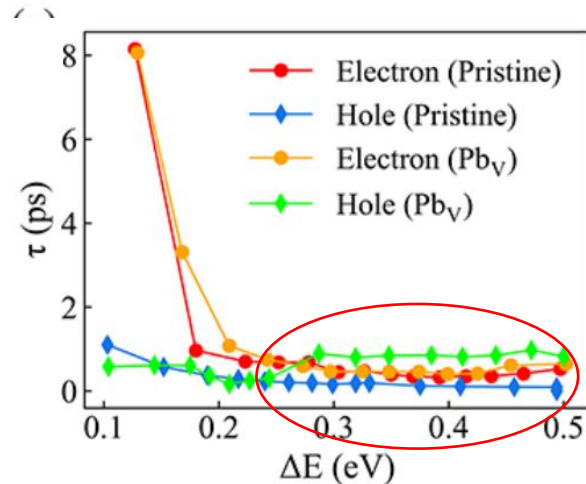
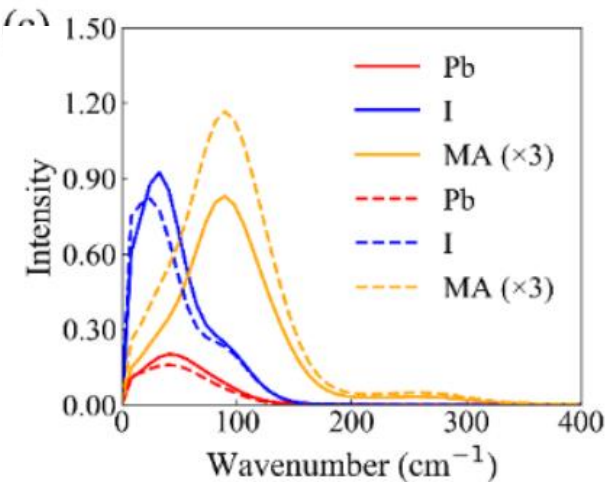
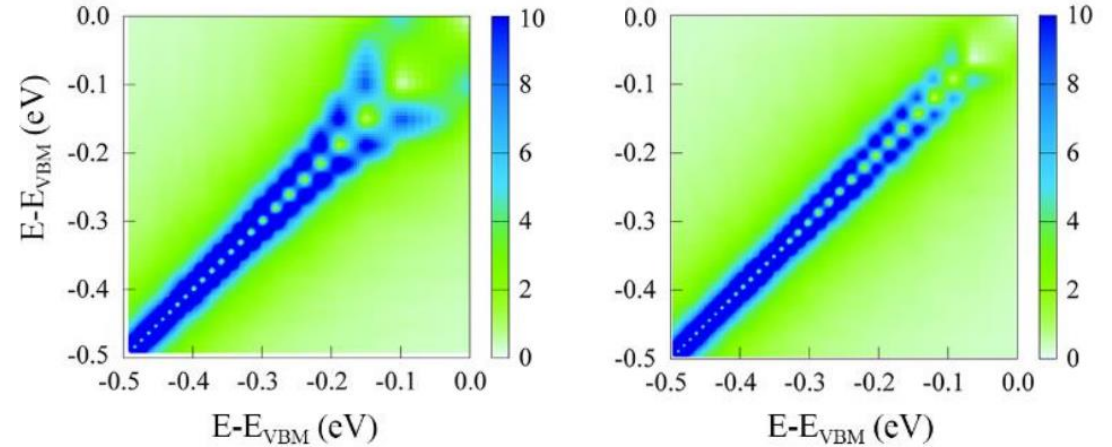
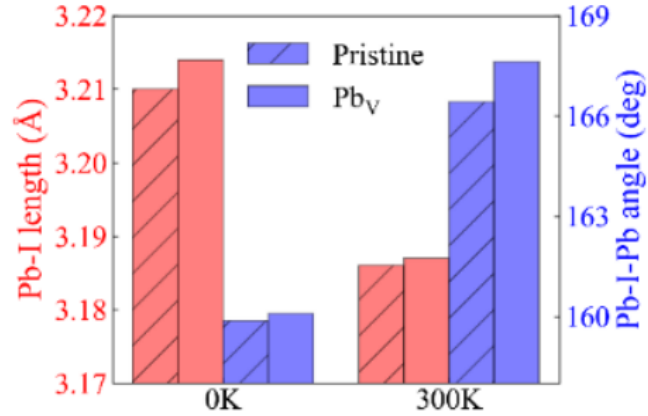
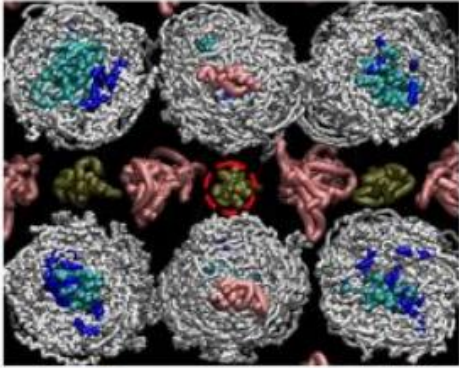


ACS Energy Lett., 2017, 2, 1270

- Hole trapping is fast, but recombination of trapped hole with free electron is slow because wavefunction overlap is small
- Hole can be trapped and de-trapped multiple times before recombining, increasing free carrier lifetimes

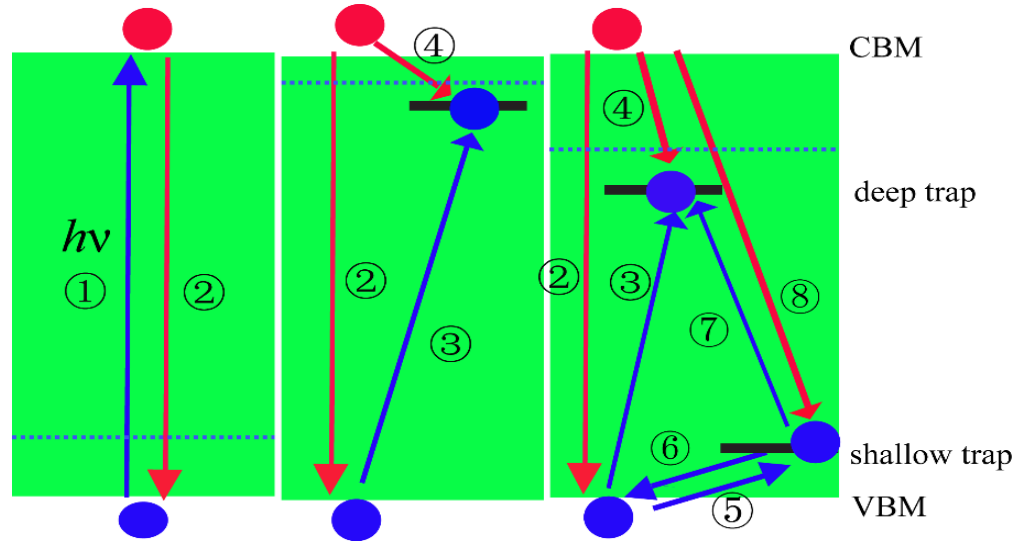


Pb Vacancy Slows Down Carrier Cooling



- Pb vacancy increase the structural ordering, decreases fluctuations of Pb and I atoms, and reduces NA couplings
- Pb vacancy introduces intraband states capable of trapping hot holes, slowing down its cooling further

Oxidization States of Iodine Vacancy

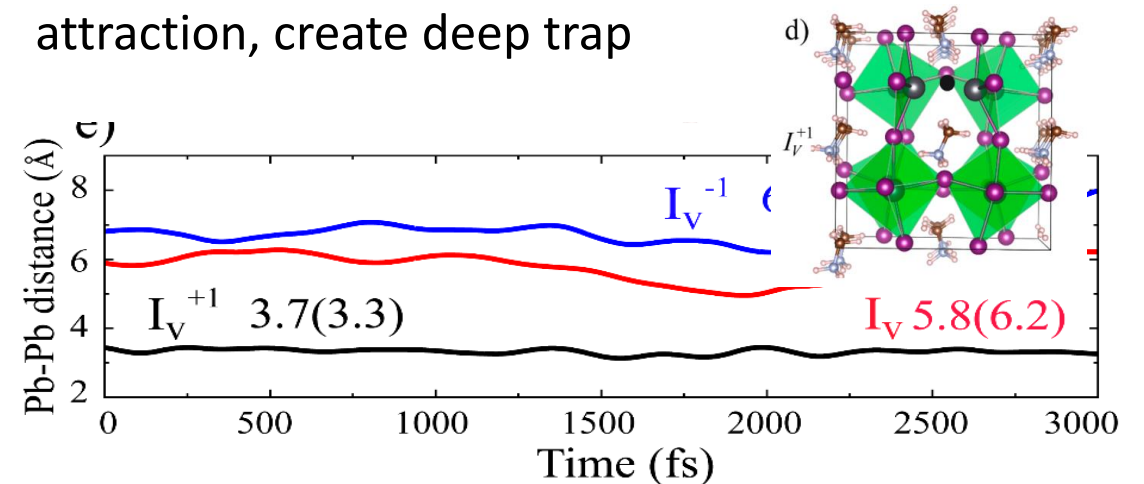


Missing I⁻: Lose an electron enlarges the Pb-Pb distance due to Coulomb repulsion, and creates no trap states

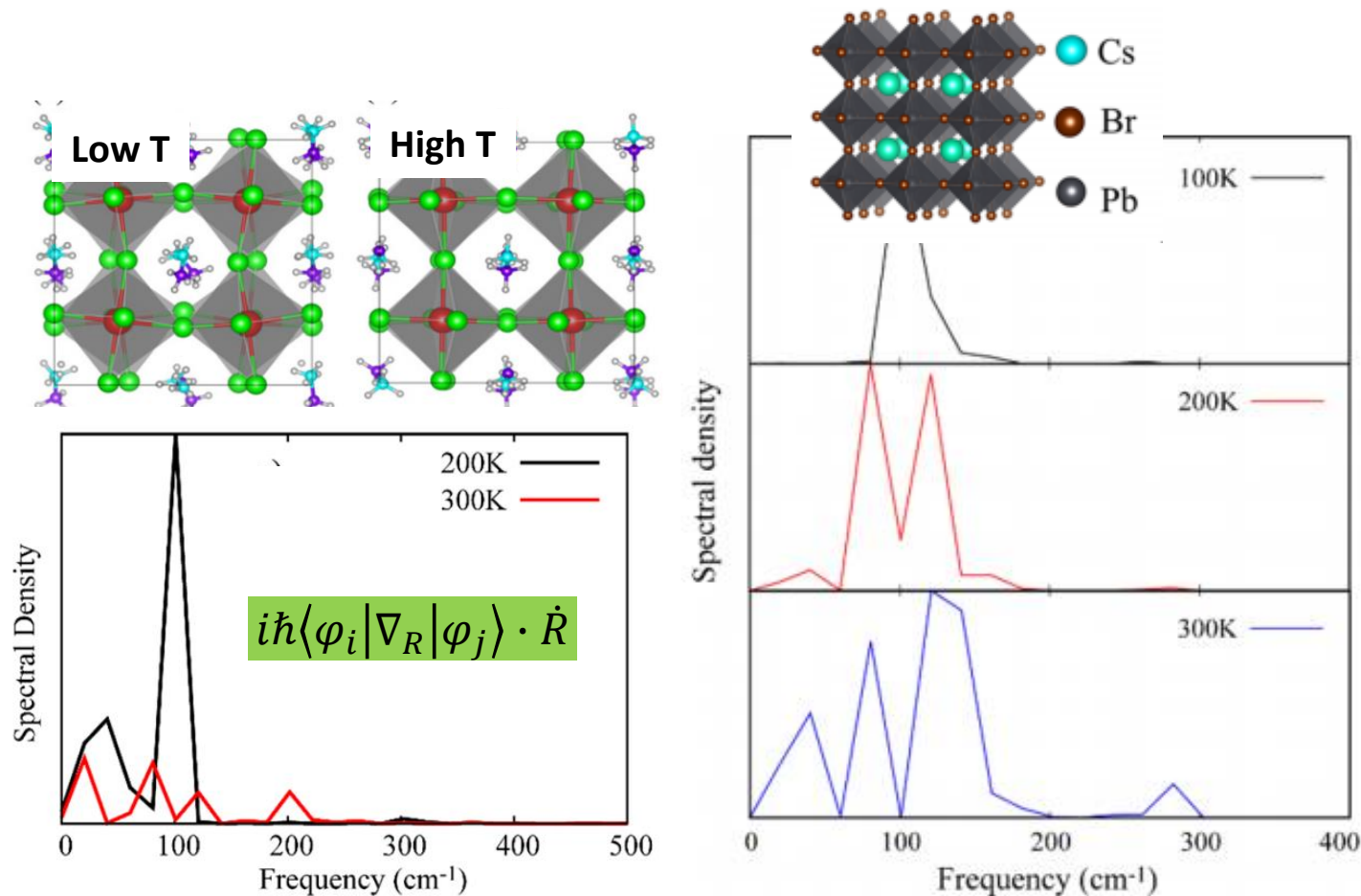
Missing I: create shallow trap

Missing I⁺: Capture of an electron shortens the Pb-Pb distance and form Pb-Pb dimer due to Coulomb attraction, create deep trap

| | Recomb. time | Mechanism |
|------------------------------|--------------|-----------------------|
| Pristine | 152ns | CBM->VBM |
| Missing I⁻ | 136ns | CBM->VBM |
| Missing I | 27ns | CBM->VBM, via trap |
| Missing I⁺ | 3ns | Sequential (via trap) |



Temperature-dependent Carrier Lifetime



| | d (Å) | θ (deg) | E_g (eV) | σ_E (eV) | NAC (meV) | T_2^* (fs) | T_1 (ns) |
|-------|---------|----------------|------------|-----------------|-----------|--------------|------------|
| 100 K | 2.975 | 170.5 | 1.48 | 0.088 | 1.14 | 7.9 | 0.89 |
| 200 K | 2.971 | 168.7 | 1.60 | 0.12 | 1.34 | 5.9 | 1.22 |
| 300 K | 2.970 | 165.8 | 1.75 | 0.15 | 1.80 | 4.7 | 1.45 |

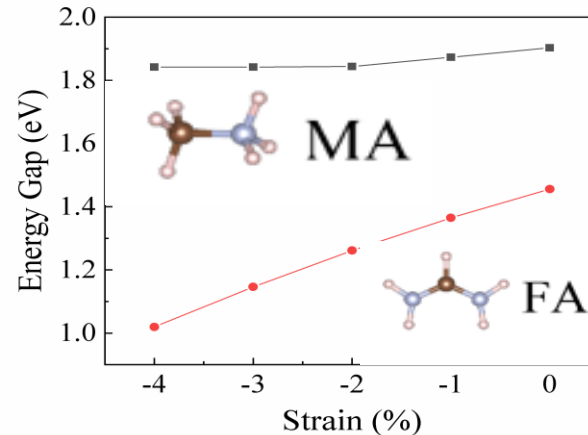
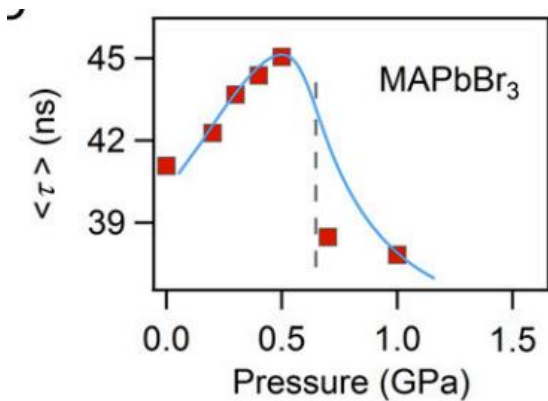
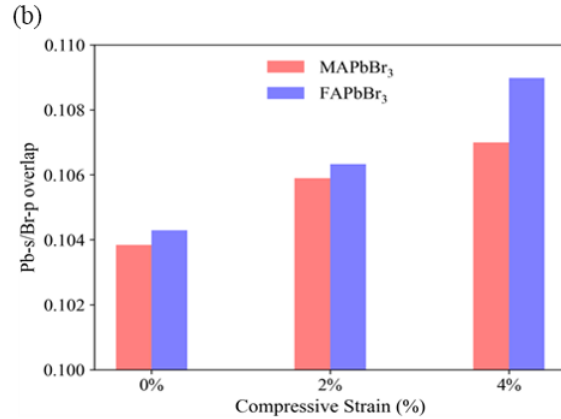
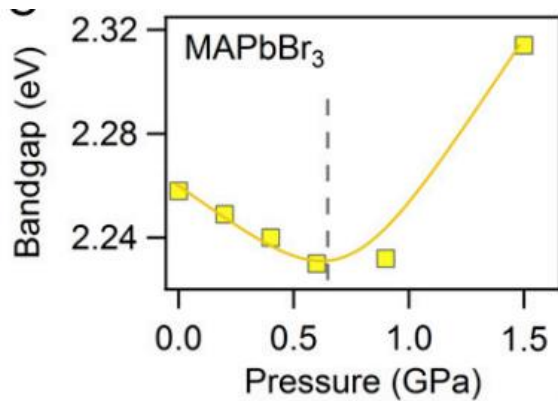
- Higher T increases **rotational disorder of organic cations** which suppresses fluctuation of Pb-I lattice in **hybrid organic-inorganic perovskite**
- Higher T activates **broad range of phonon modes**, accelerating pure-dephasing in **all-inorganic perovskite**

Inorgan. Chem. Front., 2022, **9**, 5549

J. Phys. Chem. Lett. 2019, **10**, 6219

ACS Energy Lett., 2018, **3**, 2713

Anti-correlation between Carrier Lifetime and E_g



| | | Energy Gap (eV) | NAC (meV) | Dephasing Time (fs) | Lifetime (ns) |
|---------------------|-----|-----------------|------------|---------------------|---------------|
| MAPbBr ₃ | 0 | 1.90 | 0.52 | 6.05 | 10.32 |
| | -2% | 1.85 | 0.53 | 5.32 | 12.49 |
| | -4% | 1.84 | 0.55 | 4.90 | 12.63 |
| FAPbBr ₃ | 0 | 1.46 | 0.58 | 4.93 | 0.38 |
| | -2% | 1.26 | 0.63 | 4.34 | 0.35 |
| | -4% | 1.02 | 0.66 | 3.39 | 0.30 |

- The larger band gap variations is induced by stronger Pb-s/Br-p overlap, facilitated by the larger Pb-Br-Pb angle
- Compression suppresses the fluctuations of organic cations, unlocks the Pb-Br vibration and enhance the electron-phonon interactions

Kong et al, PNAS, 2016, 113, 8910

Chem. Mater. 2020, **32**, 4707

Chem. Mater., to be submitted

Summary

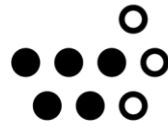
- Longer alkyl chain slows down interlayer CT
- SOC accelerates nonradiative dynamics
- Simple Hamiltonian repetition extends the NA-MD time scale
- Defects trap/de-trap free charges (softness)
- Breaking the hybridization of dangling states passivate defect states
- Disorder (unusual T and P dependence)

Acknowledgements

Collaborators

- Oleg Prezhdov (U Southern California, U.S.)
- Alexey V. Akimov (U Buffalo, U.S.)
- David Beljonne (UMONS, Belgium)
- Zhufeng Hou (CAS, China)

\$
\$
\$



Wallonie - Bruxelles
International.be



Deyang, Pingzhi, me, Zhiguo, Junguang
Jiayi, Ting, Xueying, Ning